

Coalescence of Nanoclusters and Formation of Submicron Crystallites Assisted by *Lactobacillus* Strains

Binoj Nair and T. Pradeep*

Department of Chemistry and Regional Sophisticated Instrumentation Centre,
Indian Institute of Technology, Madras 600 036, India

Received April 6, 2002; Revised Manuscript Received May 13, 2002

ABSTRACT: *Lactobacillus* strains, common in buttermilk, assist the growth of gold, silver, and gold–silver alloy crystals of submicron dimensions upon exposure to the precursor ions. Several well-defined crystal morphologies are observed. Crystal growth occurs by the coalescence of clusters, and tens of crystals are found within the bacterial contour. Crystal growth does not affect the viability of the bacteria. Crystals are presumably nucleated through nanoclusters, which are formed within as well as transported into the bacteria. Biomass with the crystals can be harvested completely. Results point to potential applications in analytical chemistry, nanotechnology, medicine, and metal ion recovery. Coalescence appears to be a route by which surface area of the crystal is reduced so that it can be effectively protected to avoid biological damage.

Introduction

Tomorrow's technology is going to depend on nanostructured metals¹ and semiconductors.² It is predicted that the impact of this technology will be felt greatly at the interface of chemistry and biology.³ The desire to synthesize materials using efficient and green chemistry approaches is considerable, which has led to the use of microorganisms. Although efforts directed toward nanomaterials are recent, metal ion interaction with prokaryotic species has been one of the focal points of research for a long time.⁴ Bacteria have been known to enrich ions,⁵ synthesize magnetite crystals,^{5,6} reduce Ag⁺ into metal particles,⁷ form nanoparticles^{5,8} as well as octahedral gold⁹ containing S and P, and recently, prepare ceramic to metal composites¹⁰ (cermets). Formation of minerals by unicellular and multicellular organisms has long been recognized; the synthesis of siliceous materials¹¹ by diatoms and the preparation of gypsum and calcium carbonate¹² by S-layer bacteria are some of the examples. Single-crystalline semiconducting particles such as CdS have been synthesized in algae.¹³ The most recent addition into this biosynthesis approach is the reduction of gold and silver by fungi.¹⁴

Variety and diversity of this chemistry suggest numerous possibilities with other, more common microorganisms. Herein we report the growth of gold, silver, and gold–silver alloy crystals with well-defined morphologies assisted by most common *Lactobacillus* strains found in buttermilk, when exposed to appropriate ions. Accumulation of metals occurs to such an extent that about 35% of the dry bacterial biomass harvested is metal. The size of the crystals can be controlled to a large extent, although varying shapes are observed. The biocolloidal suspension formed this way is stable. Presence of the metal does not affect the viability of the bacteria. The biomass along with the crystals can be harvested completely by ultrafiltration. The results point to several applications.

Experimental Procedures

A total of 0.5 L of home delivered milk was boiled, cooled, and mixed with 10 mL of standard buttermilk, curdled at 27 °C for 24 h, and the whey was collected by coarse filtration (Whatman 40). All the reactions were done in the laboratory atmosphere in glass apparatus. The filtrate was pale yellow in appearance, and the pH was typically 4.4. The presence of lactic acid bacteria in the supernatant was ascertained with an optical microscope. HAuCl₄ and AgNO₃ were from CDH chemicals, with rated purity of 99%. To 5 mL of this solution taken in a test tube, 2 mg of HAuCl₄·3H₂O was added and kept in the laboratory under ambient conditions. The solution became purple in about 12 h. A purple mass gets deposited at the bottom of the test tube after 24 h. Within 3 days, all of the gold containing material deposited, forming a violet film, and the solution became colorless. In the case of Ag, 1 mg of AgNO₃ was added to 5 mL of whey and kept in the laboratory overnight. The solution became pale brown and after 2 days, precipitation was noticed. The biomass containing silver precipitated after 3 days making the solution colorless. All preparations were conducted in the laboratory ambience; effect of light in the synthesis was not investigated. Citrate covered gold clusters of 20–30-nm diameter were prepared using the sodium citrate route.¹⁵ Sodium citrate was purchased from Aldrich.

UV/VIS measurements were done with a Varian Cary 5 spectrometer. X-ray diffractograms were taken with a Siemens diffractometer with CuK α radiation. FT-Raman spectra were measured with Bruker FRA106 FT-Raman instrument with Nd:YAG (1064 nm) excitation. TEM measurements were done with a Philips CM12 120 keV instrument. A dilute suspension of the material in distilled water was mildly sonicated for 30 s. A drop of it taken with a GC syringe was placed onto carbon coated Cu grids, with a mesh size of 40 \times 40 μ . The grid was left for slow drying in air. Mild sonication was not responsible for the phenomena observed as checked by an independent experiment. The beam energy or duration of exposure did not show any visible effect on the quality of the pictures. Several of the specimens prepared this way were repeatedly measured, and the picture quality was reproducible. No additional heavy metal staining or sample preparation was found necessary. To remove bacteria, ultrafiltration was done with Sartorius 0.2 micron (cellulose acetate) membrane filters with associated accessories. The filtrate was used as such. The collected bacterial growth was washed twice with distilled water and dried in air for XRD. The sample was weighed after drying in an oven at 110 °C. A portion of the dried membrane was

* To whom correspondence should be addressed. Fax: ++91-44-257 0509/0545. E-mail: pradeep@iitm.ac.in.

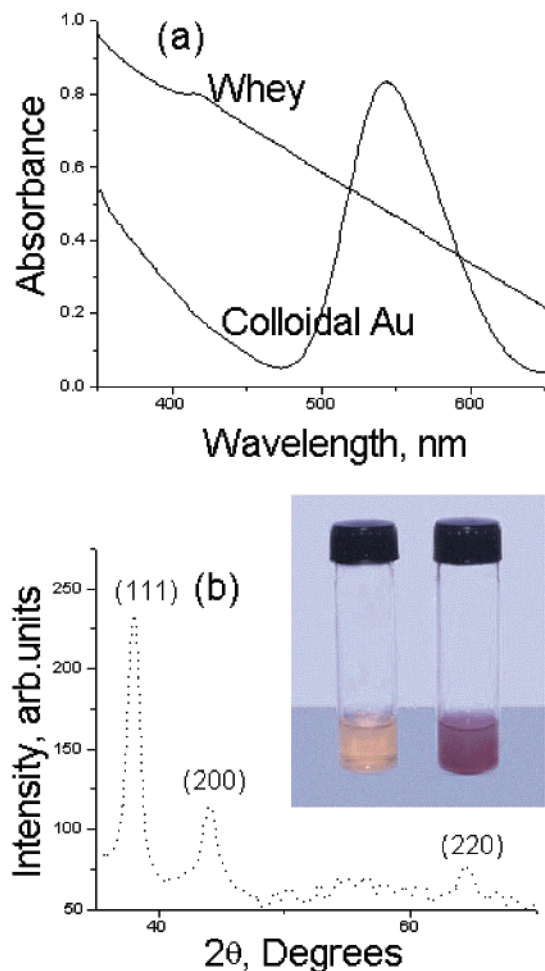


Figure 1. (a) UV/VIS absorption spectrum of colloidal Au prepared with whey. The reference whey spectrum is also shown. The spectrum of the colloid shows a longer wavelength structure as shown in Figure 3. (b) XRD of the purple mass showing (111), (200), and (220) reflections of bulk fcc Au. Photograph of two bottles containing whey soon after adding HAuCl_4 (left) and after 12 h (right) is shown in the inset.

mounted in the XPS (VG ESCALAB MkII) chamber and analyzed with unmonochromatized AlK_α radiation.

Results and Discussion

The UV/VIS spectrum of the Au sample after 12 h of exposure showed a well-defined surface plasmon band centered around 540 nm characteristic of colloidal gold (Figure 1a). Various studies have established that the surface plasmon resonance band of gold appears around this value for colloidal gold in the size range of 30 nm, and the exact position depends on a number of factors such as the dielectric constant of the medium, size of the particle, etc. Solution at this stage becomes purple in color (Figure 1b, inset) characteristic of colloidal gold. Formation of elemental gold is clear from the X-ray powder diffractogram of the deposited biomass (Figure 1b). Sharp reflections due to (111), (200), and (220) were the only features observed corresponding to bulk fcc Au. Peak-widths were narrower than the typical thiol protected nanoclusters,¹⁶ indicating that the particle size is much larger. The precipitated material after heating to 200 °C formed elemental gold. An interesting aspect is that the gold film formed on a glass plate (after heating at 200 °C) was of preferential (111) orientation.

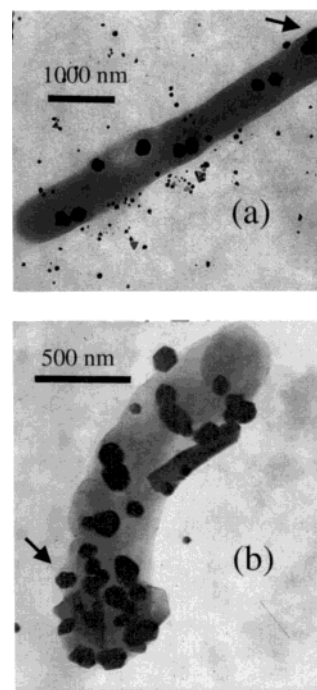


Figure 2. Electron micrographs of the growth of gold crystals in *Lactobacillus* strains. (a) Shows a *Lactobacillus* strain with several gold crystals. The crystals within the bacterial contour are much larger than the clusters outside. (b) Another bacterium with more crystals. Several crystal morphologies are manifested. Arrows point to regions where the cell wall is being pushed with the edges of the crystals.

A drop of the solution after reaction for 12 h was placed on carbon coated Cu grids for transmission electron microscopy. Two TEM micrographs are shown in Figure 2. In Figure 2a, we see a rod-shaped bacterium. The darker regions are gold crystals as revealed by electron diffraction (see Supporting Information). Two kinds of size ranges are seen for gold crystals, those in the range of 20–50 nm and those above 100 nm (referred to as clusters and crystals, respectively, subsequently). Clusters are present within and outside the bacterial contour, while the crystals are seen exclusively within the bacterial contour. Various crystal morphologies are manifested; mostly hexagonal, but triangular and other shapes are also observed. It is noted that most of the clusters are fairly uniform in size. Growth of the crystals happens such that most of the bacterial cell contour is consumed by the crystals (Figure 2b). It is also clear that several of the *Lactobacillus* strains show crystal growth in them. While the growth is predominantly seen in lactobacilli, other organisms, especially cocci also showed gold crystals in them. In Figure 2, it is important to see that bacterial cell wall is pushed during the crystal growth (see the arrows). It appears that growth makes the crystals come near the inner surface of the bacteria. Even after the bacterium ruptures, the crystals preserve the bacterial contour (see Supporting Information). All of these suggest that crystal growth occurs inside the cell; involvement of the surface is not ruled out, however.

Certain experiments were done to understand the observed phenomena in greater detail. (a) The biomass precipitated during crystal growth was found to be active for curdling. Curd prepared this way was purple

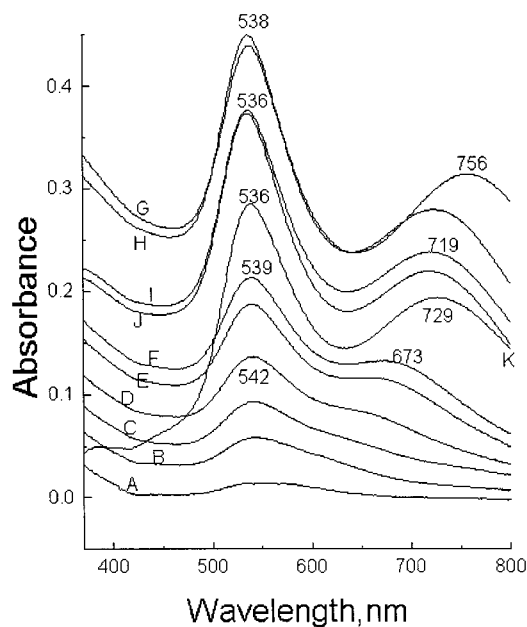


Figure 3. Time dependence of the absorption spectrum after addition of HAuCl_4 (1 mg of $\text{HAuCl}_4 \cdot 3\text{H}_2\text{O}$ in 5 mL of clear whey after coarse filtration). A, B, C, D, E, F, G, H, I, J, and K are 1, 2, 3, 4, 8, 16, 24, 48, 56, 64, and 72 h after the addition of HAuCl_4 . The intensities start decreasing after G as precipitation of the biomass occurs.

in color. (b) The supernatant after bacteria removal by ultrafiltration manifested cluster growth upon addition of HAuCl_4 , no crystals were seen, and these were confirmed by TEM (also, no bacteria were seen). (c) The supernatant after removal of precipitated gold clusters along with the biomass was colorless and was also found to be effective for cluster growth. (d) Independent studies with L-lactic acid, a constituent of whey, showed that it could reduce gold at the laboratory temperature. However, large crystals were seen only in the presence of live bacteria; (e) Whey after boiling for 10 minutes did not show them, although nanoclusters were observed. These studies showed that lactic acid bacteria are necessary for crystal growth and also that other bacterial contamination did not occur during the experiment.

While it is evident that the chemistry involved is complex, we rationalize the observation in the following way. Accumulation and reduction of Au^{3+} inside bacterial cells such as *Bacillus subtilis* 168 have been noted before.⁹ It is evident that the gold ions can be reduced by acids present in the medium. Sugars are also known to cause reduction. Thus, it is likely that most, not all, of the initial nucleation of clusters occurs extraneous to the bacterial cells. Note that reducing species are present inside the bacteria, and ion transport into the cell is a known phenomenon. Subsequently, the formed nanoclusters grow within the cells, which appears to involve coalescence (see below). The foregoing conjecture is supported by time-dependent absorption spectroscopic measurements (Figure 3). In the initial stages of particle growth, only a single plasmon peak is manifested. Gradually, a peak above 600 nm evolves that progressively shifts to red; also note that the peak-width of this structure increases with time. An important aspect to note is that the peak at ~ 540 nm remains at the same value. The longer wavelength absorption corresponds

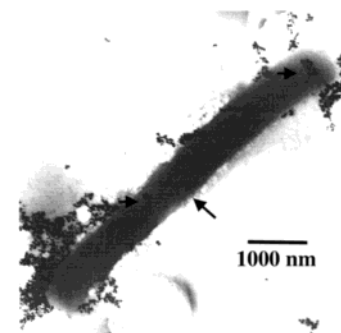


Figure 4. TEM image illustrating coalescence inside the bacteria. The smaller particles of about 25 nm are made outside the bacteria. Aggregation of these clusters is observed, yet they preserve their identity. Within the bacteria, coalescence leads to larger crystallites. Some of them are marked with arrows. Note the shape of the crystals formed inside the bacterium showing contours arising out of the coalescence of clusters.

to the plasmon of larger particles in the extinsic size range where the position red shifts and the peak-width increases with dimension.¹⁷ In this size range, the size dependence enters through a full expression of Mie's theory. Beyond 24 h, part of the colloidal material precipitates, contributing to a reduction in the background intensity. This peak is sensitive to the changes in the medium; as time progresses a shift in the peak maximum is observed. Note that this second peak cannot be attributed to nanorods of various aspect ratios as such species have different absorption spectra.¹⁷ We also see no nanorods in our TEM (Figure 2).

Evolution of absorption spectra also indicates a nucleation and growth mechanism. While it is known that the reduction of Au^{3+} ions is possible with sugars and enzymes at the cell wall leading to gold atoms, growth of the crystals requires the buildup of these atoms over a nanocluster nucleus. Coming to the clusters formed extracellularly, they are likely to be protected with charged molecular species such as carboxylates through electrostatic interactions just as in monolayer protected clusters.¹⁶ These interactions also appear to make it possible for the clusters to transfer into the bacterial cell. Note that the bacterial cell wall is negatively charged, and electrostatic interaction of the species there with gold clusters will be favored, just as in the case of anion protected clusters. Diffusion of smaller clusters of nanometer dimensions through the cell wall is therefore, expected to occur. To check this hypothesis of nucleation and transfer of clusters, whey was added to citrate protected clusters prepared previously. TEM analysis after 12 h showed clusters within the bacterial contour, but they remain largely of their original size; some aggregation was noticed, however. Figure 4 shows that while smaller clusters are predominantly seen outside the bacterium, larger crystallites are seen within. Aggregation and fusion of clusters around these crystallites are also observed. Clusters outside also show a tendency to aggregate, yet they retain their identity. The fact that coalescence occurs within bacteria and not outside points to a need to reduce the exposed surface area of the clusters.

The size distribution and kinetics of growth are affected by various factors. Among them, pH was found to be important. For a pH of 4, the larger particles were

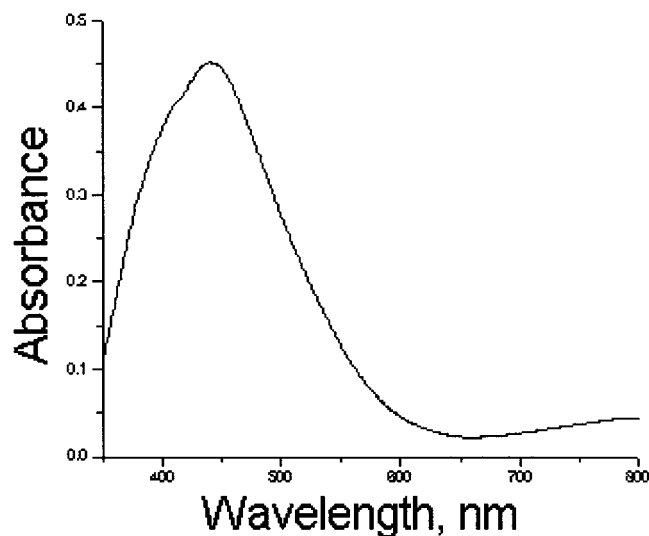


Figure 5. UV/VIS absorption spectrum of a bacterial colloid of silver showing well-defined surface plasmon resonance band centered at 439 nm. Shift from the characteristic silver value of 420 nm for alkanethiol protected silver clusters in organic media is expected. The spectrum shows asymmetry in the blue region of the plasmon resonance, attributed to absorption of various organic species at the surface.

observed early. Particles corresponding to an absorption maximum of ~ 650 nm and beyond were seen 3 h after Au^{3+} exposure. It is also seen that beyond a time of 10 h, intensity due to the larger particles grows, while that of the smaller particles diminishes. This obviously means that the larger crystallites are growing at the expense of clusters. We attribute this to the coalescence of clusters within the bacteria. It appears that the growth is strongly influenced by the chemical environment of the medium. When lactic acid bacteria were removed from whey by ultrafiltration, larger crystallites were not observed in the UV/VIS spectrum recorded after 24 h. TEM did not show bacteria and larger crystallites (all spectra in the Supporting Information).

Silver-based clusters are formed with AgNO_3 . The preparation involved mixing whey with AgNO_3 . The solution becomes brown in color within 12 h, and the UV/VIS absorption spectrum (Figure 5) indicates a well-defined surface plasmon resonance peak at 439 nm. The structure is much narrower than the typical alkanethiol protected silver nanoclusters^{16b} indicating that they are large colloids. The asymmetry in the high energy side of the band is attributed to electronic excitations of the surface bound ligands.¹⁸ The absorption spectrum evolves gradually over a period of 24 h; during this time, aggregation leads to complete precipitation of the biomass along with colloids, and the solution gradually becomes colorless. Unlike in the case of gold, no long wavelength peak is observed. Biosorption and bioreduction of AgI by *Lactobacillus Sp. A09* have been reported by Fu et al.¹⁹

TEM image of a bacillus is shown in Figure 6. The bacterial contour and cell wall are clearly observable. It is clear that crystal growth forces the cell wall to be pushed, indicating that the particle growth is occurring mostly inside the bacterium. The darker regions seen are crystalline, as revealed by selected area electron diffraction (see Supporting Information). The electron diffraction pattern does not match with atomic silver,

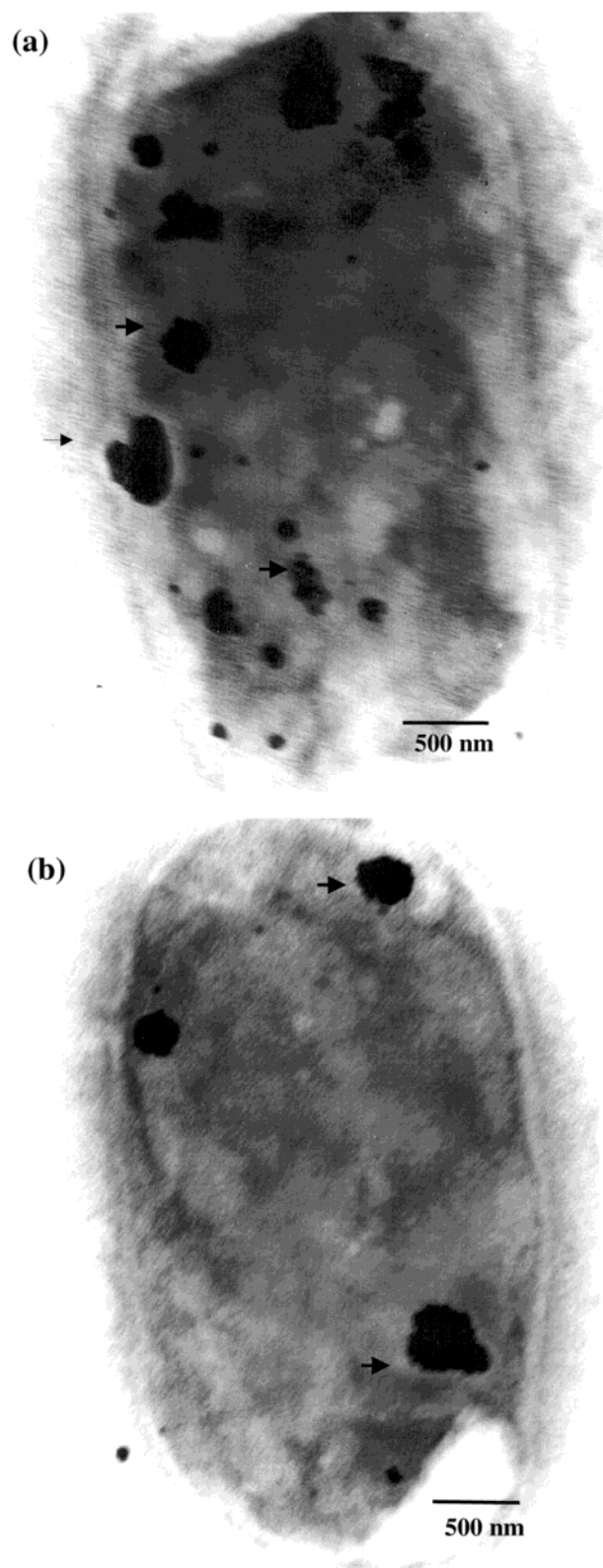


Figure 6. (a) TEM of a *Lactobacillus* strain with silver clusters and large crystallites. Several morphologies are noted. See the projection of the cell wall as a result of cluster growth (dotted arrow). (b) TEM illustrating coalescence of clusters and the formation of large crystallites. Most of the morphologies observed are clearly due to such coalescence; some are marked with arrows.

and it appears that bulk composition could be significantly different from elemental silver, as observed in

the case of *Pseudomonas stutzeri* AG259⁷ where monoclinic Ag₂S was seen within the bacteria. XRD of the air-dried biomass, in our case, does not agree with either monoclinic or cubic Ag₂S, and the product appears to be a composite with a silver rich core with an external shield of chemically modified silver, in accordance with the observed surface plasmon resonance feature. The sample upon heating to 100 °C for 5 h results in a metallic silver film.

The smallest particles observed are in the range of 15 nm, while the largest are around 500 nm along one axis. While the smallest particles are separated, the larger ones show clear aggregation. For the larger particles, several morphologies are observed. It is important to note that the surface morphology of these crystals is distinctly different from gold, where sharp contours are observable for all the crystals, presumably because of the thick protecting layer. Most of the larger crystallites have smaller particles around them, and a few are marked in Figure 6. Growth of particles is clearly observable in Figure 6b, where larger particles show well-defined protrusions due to the coalescing clusters. Faceted morphologies could arise subsequently. It appears that the time scales of coalescence and subsequent annealing are slower for silver, making intermediate structures observable.

The valence states of the products were investigated by X-ray photoelectron spectroscopy. Au 4f_{7/2} appears at 84.0 eV binding energy, characteristic of metallic Au. Ag 3d_{5/2} is seen at 368.0 eV, again characteristic of metallic Ag. Complete reduction of the metal ions is clear from the XPS data. The spectra show very little inelastic background suggesting that the molecular shell covering the surface is much thinner than the inelastic mean free path of the electrons. XPS showed all the other expected elements such as C, O, S, N, and P. Data in the Au 4f and Ag 3d regions of Au and Ag bacterial materials are given in Supporting Information.

Although it is premature to comment on the mechanistic details, we suggest the following tentative explanation. It is suggested that the periplasmic silver binding proteins partially or completely bind silver at the cell surface, protecting the cytoplasm from toxic concentrations.²⁰ Protection from larger quantities of silver require a reduced surface area for the clusters, so that adequate silver binding proteins are available, which can effectively protect the surface to make the cell survive. This might be the driving force for the crystal growth.

Silver is toxic to most microbial cells. However, there are several instances where silver accumulation has been reported, even to the extent that industrial silver recovery is proposed.⁵ Examples include, *Pseudomonas stutzeri* AG259 forming metallic silver and silver metal composites containing S and P, as noted before.⁷ The role of capsular polymers in the protection of bacterial cells from toxic metals is known.²¹ Reduction in free metal ion concentration due to complexation is the likely reason for tolerance.²⁰ Cluster formation and their aggregation leading to microcrystals with appropriate surface protection may be looked at from this perspective.

The approach discussed above can be extended for the preparation of alloy clusters also. Appropriate quantities

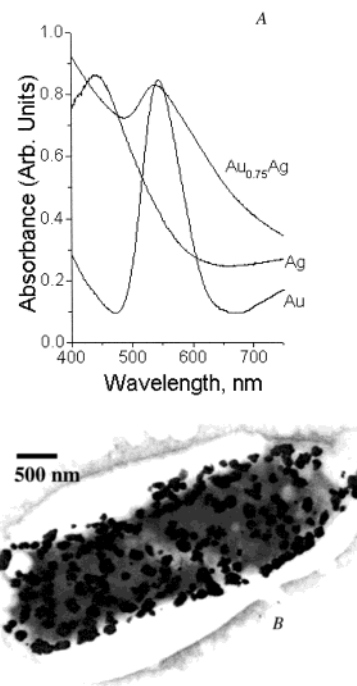


Figure 7. (A) Comparison of the UV/VIS absorption spectra of bacterial colloids of pure Au and Ag with an alloy colloid of starting composition AuAg_{0.75}. The peak maxima are 547, 439, and 537 nm for Au, Ag, and AuAg_{0.75}, respectively. Note that there is no peak due to Ag colloid in the alloy. The spectra have been moved vertically as there is shift in baseline from sample to sample. (B) TEM of a bacterium with alloy crystallites. [111] zone axis was seen in electron diffraction. Smaller crystallites are seen outside the bacteria as well.

of HAuCl₄·3H₂O and AgNO₃ were mixed with 5 mL of the supernatant so as to form a millimolar solution. We studied several compositions from Au₁Ag₀ to Au₀Ag₁. All the compositions formed colloidal solutions characterized by their sharp surface plasmon resonance feature. In the case of alloys, the plasmon peak is between silver and gold, shifted more toward gold (Figure 7a).²² No plasmon resonance due to pure metal clusters is observed in these preparations ruling out core-shell structures. In TEM, it is clear that crystallites of 100–300 nm along one of the axes cover the periplasmic space of the bacteria, occupying nearly all of the available surface area (Figure 7b). The cell wall is also observable. The biomass can be harvested completely as complete precipitation of the material occurs over a period of 72 h.

We felt that it is important to look at potential applications of noble metals in the bacterial environment. An immediate application would be in the chemical mapping of bacteria using surface enhanced Raman spectroscopy (SERS). As noble metal surfaces can enhance Raman signals and many biological species have strong anchoring sites which could bind on these surfaces, the technique should be potentially useful. To explore this application, we recorded the FT-Raman spectra of thin films of the bacterial material after Au, Ag, and Au_{0.75}Ag alloy crystal growth, prepared on a glass substrate. All the spectra (Figure 8) are largely similar, showing only a few characteristic frequencies at 2920, 1103, and 564 cm⁻¹, which can be assigned immediately to C–H, C–C, and C–S stretching frequencies. As the spectrum of a complex mixture such

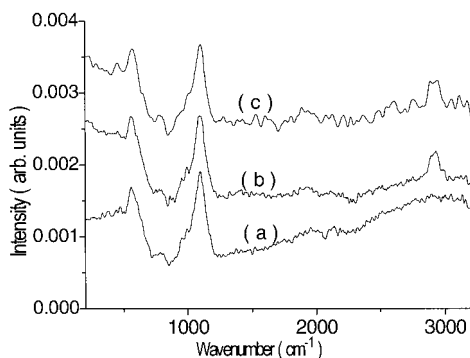


Figure 8. FT-Raman spectra of the bacterial biomass with (a) Au, (b) Ag, and (c) alloy crystals. Peaks are observed at 564, 1103, and 2920 cm^{-1} . For Au, the peak at 2920 cm^{-1} is not observed.

as they reveals only a set of characteristic features, we attribute them to the species adsorbed on the microcrystal surface. Absence of a C–H stretch in Figure 8a also suggests this, explained as due to orientational changes of the molecules on this surface as SERS is sensitive to adsorbate structure.²³ The difference between the three spectra in this region, while all the features remain the same, supports the suggestion. Although these studies can be extended further, application of this methodology in understanding biological processes is demonstrated.

To conclude, common *Lactobacillus* strains found in buttermilk assist the growth of microscopic gold, silver, and gold–silver alloy crystals of well-defined morphology. Crystal growth appears to occur via intracellular reduction of the metal ions, while most of the smaller metal clusters which nucleate the growth are diffused into the cell from the reducing outside medium. They are also formed within the cell. The bacteria preserve their viability even after crystal growth. The method suggests interesting possibilities in nanomaterial synthesis, metal ion recovery, and medical applications including rheumatology and drug delivery. Immediate application seems to be in the in situ investigation of biomolecules using SERS. We are aware that thin sections have to be examined to definitively prove that processes are happening inside the cells. We are right now involved with studies on pure lactobacilli and other strains to explore the process in greater detail.

Acknowledgment. The metal cluster research program in our laboratory is supported by the Department of Science and Technology and Council of Scientific and Industrial Research, Government of India. B.N. thanks Inter University Consortium for DAE facilities for a research fellowship. T.P. thanks professors P. T. Manoharan, T. S. Chandra, and K. Lalitha for discussions; Dr. Bindhu Varughese, University of Notre Dame, USA for XPS; Prof. S. Vasudevan, Indian Institute of Science, Bangalore, for SERS; and Mrs. Kanjanamala for TEM measurements.

Supporting Information Available: Electron diffraction patterns of Au and Ag crystallites, TEM image of the gold crystals preserving the ruptured bacterial contour, time evolu-

tion of the absorption spectra of Au microcrystals, and XPS in the Au 4f and Ag 3d regions. This material is available free of charge via the Internet at <http://pubs.ac.org>.

References

- (1) Schmid, G.; Chi, L. F. *Adv. Mater.* **1998**, *10*, 515; Schmid, G. in *Nanoscale Materials in Chemistry*; Klabunde, K. J., Ed., Wiley-Interscience: New York, 2001; pp 15–59.
- (2) Pileni, M. P. in *Nanoscale Materials in Chemistry*; Klabunde, K. J., Ed., Wiley-Interscience: New York, 2001; pp 61–84 and references therein.
- (3) Roco, M. C.; Bainbridge, W. S. *Societal Implications of Nanoscience and Technology*, NSET Workshop Report, March 2001, available at www.nano.gov.
- (4) Simkiss, K.; Wilbur, K. M. *Biomimetalization*; Academic Press: New York, 1989; Mann, S., Ed. *Biomimetic Materials Chemistry*; VCH: New York, 1996.
- (5) Beveridge, T. J.; Doyle, R. J., Ed. *Metal Ions and Bacteria*; Wiley: New York, 1989.
- (6) Spring, H.; Schleifer, K. H. *System. Appl. Microbiol.* **1995**, *18*, 147; Dickson, D. P. E. *J. Magn. Magn. Mater.* **1999**, *203*, 46.
- (7) Klaus, T.; Joerger, R.; Olsson, E.; Granqvist, C.-G. *Proc. Natl. Acad. Sci. U.S.A.* **1999**, *96*, 13611–13614; Klaus, T.; Joerger, R.; Olsson, E.; Granqvist, C.-G. *Proc. Trends Biotechnol.* **2001**, *19*, 15–20.
- (8) Fortin, D.; Beveridge, T. J. in *Biomimetalization. From Biology to Biotechnology and Medical Applications*; Baeuerlein, E., Ed.; Wiley-VCH: Weinheim, 2000.
- (9) Southam, G.; Beveridge, T. J. *Geochim. Cosmochim. Acta* **1996**, *60*, 4369–4376.
- (10) Joerger, R.; Klaus, T.; Granqvist, C.-G. *Adv. Mater.* **2000**, *12*, 407–409.
- (11) Mann, S. *Nature* **1993**, *365*, 499–505; Oliver, S.; Kupermann, A.; Coombs, N.; Lough, A.; Ozin, G. A. *Nature* **1995**, *378*, 47.
- (12) Pum, D.; Sleytr, U. B. *Trends Biotechnol.* **1999**, *17*, 8–12; Sleytr, U. B.; Messner, P.; Pum, D.; Sara, M. *Angew. Chem.* **1999**, *111*, 1099; *Angew. Chem., Int. Ed. Engl.* **1971**, *10*, 230.
- (13) Dameron, C. T.; Reese, R. N.; Mehra, R. K.; Kortan, A. R.; Carrol, P. J.; Steigerwald, M. J.; Brus, L. E.; Winge, D. R. *Nature* **1989**, *338*, 596–597.
- (14) Mukherjee, P.; Ahmad, A.; Mandal, D.; Senapati, S.; Sainkar, S. R.; Khan, M. I.; Ramani, R.; Parischa, R.; Ajayakumar, P. V.; Alam, M.; Sastry, M.; Kumar, R. *Angew. Chem., Intl. Ed.* **2001**, *40*, 3585–3588; Mukherjee, P.; Ahmad, A.; Mandal, D.; Senapati, S.; Sainkar, S. R.; Khan, M. I.; Parischa, R.; Ajaykumar, P. V.; Alam, M.; Kumar, R.; Sastry, M. *Nano Lett.* **2001**, *1*, 515–519.
- (15) Handley, D. A. *Colloidal Gold: Principles, Methods and Applications*; Hyat, M. A., Ed.; Academic Press: San Diego, CA, 1989; Vol. 1, pp 13–32.
- (16) Brust, M.; Walker, M.; Bethell, D.; Schiffrin, D. J.; Whyman, R. *J. Chem. Soc., Chem. Commun.* **1994**, 801–802; Sandhyarani, N.; Resmi, M. R.; Unnikrishnan, R.; Ma, S.; Vidyasagar, K.; Antony, M. P.; Panneer Selvam, G.; Visalakshi, V.; Chandrakumar, N.; Pandian, K.; Tao, Y.-T.; Pradeep, T. *Chem. Mater.* **2000**, *12*, 104–113.
- (17) Link, S.; El-Sayed, M. A. *J. Phys. Chem. B* **1999**, *103*, 8410–8426.
- (18) George Thomas, K.; Kamat, P. V. *J. Am. Chem. Soc.* **122**, 2000, 2655–2656.
- (19) Fu, J. K.; Liu, Y. Y.; Gu, P. Y. et al. *Acta Phys-Chim. Sin.* **2000**, *16*, 779–782.
- (20) Geesey, G. G.; Jang, L. In *Metal Ions and Bacteria*; Beveridge, T. J.; Doyle, R. J., Ed.; Wiley: New York, 1989; Ch 11, pp 328–9.
- (21) Bitton, G.; Friehofer, V. *Microb. Ecol.* **1978**, *4*, 119.
- (22) Sandhyarani, N.; Pradeep, T. *Chem. Mater.* **2000**, *12*, 1755–1761.
- (23) Murthy, K. V. G. K.; Venkataramanan, M.; Pradeep, T. *Langmuir*, **1998**, *14*, 5446–5456.